

## Effects of short-range order on electronic properties of Zr-Ni glasses as seen from low-temperature specific heat

D. M. Kroeger, C. C. Koch,\* J. O. Scarbrough, and C. G. McKamey

*Metals and Ceramics Division, Oak Ridge National Laboratory, Oak Ridge, Tennessee 37830*

(Received 15 August 1983)

Measurements of the low-temperature specific heat  $C_p$  of liquid-quenched Zr-Ni glasses for a large number of compositions in the range from 55 to 74 at. % Zr revealed an unusual composition dependence of the density of states at the Fermi level,  $N(E_F)$ . Furthermore, for some compositions the variation of  $C_p$  near the superconducting transition temperature  $T_c$  indicated the presence of two superconducting phases, i.e., two superconducting transitions were detected. Comparison of the individual  $T_c$ 's in phase-separated samples to the composition dependence of  $T_c$  for all of the samples suggests that amorphous phases with compositions near 60 and 66.7 at. % Zr occur. We discuss these results in terms of an "association model" for liquid alloys (due to Sommer), in which associations of unlike atoms with definite stoichiometries are assumed to exist in equilibrium with unassociated atoms. We conclude that in the composition range studied, associate clusters with the compositions  $Zr_3Ni_2$  and  $Zr_2Ni$  occur. In only a few cases are the clusters sufficiently large, compared with the superconducting coherence length, for separate superconducting transitions to be observed. The variation of  $N(E_F)$  with composition is discussed, as well as the effects of this chemical short-range ordering on the crystallization behavior and glass-forming tendency.

### I. INTRODUCTION

In contrast to metal-metalloid glasses, transition-metal-transition-metal glasses can often be formed over wide composition ranges, and thus provide an opportunity for the study of properties as a function of composition. There has been a growing interest in the electronic properties of glassy alloys consisting of an early transition metal (ETM) and a late transition metal (LTM). Photoemission spectroscopy studies<sup>1-5</sup> of a number of such binary glasses have revealed some general features about their valence-band structures. For example, many such alloys (including Zr-Ni) exhibit valence bands characterized by a two-peak structure. The high-binding-energy peak has been identified with the  $d$  states of the LTM (Ni), and the peak near the Fermi level with  $d$  states of the ETM (Zr). The binding-energy difference between LTM and ETM sites tends to increase with the difference in group number between the constituents.<sup>4</sup> Kübler *et al.*<sup>6</sup> have concluded from comparisons of photoemission spectra with band-structure calculations for ordered alloys of similar stoichiometry, that the electronic structure of the glass is similar to that of an ordered close-packed state. They attribute the large shifts observed in core-level binding energy for the LTM to hybridization of the  $d$  states of the alloy constituents, and to charge transfer between unlike atoms.

The density of states at the Fermi level  $N(E_F)$  tends to be dominated by the  $d$  states of the ETM. Thus,  $N(E_F)$  should increase with the concentration of the ETM. Recent determinations of  $N(E_F)$  as a function of concentration from low-temperature specific-heat measurements<sup>7,8</sup> and from superconducting property measurements<sup>9,10</sup> of ETM-LTM glasses confirm this conclusion. Altounian and Strom-Olsen<sup>9</sup> studied the electronic properties as a

function of composition of the binary metallic glass systems Zr-Cu, Zr-Ni, Zr-Co, and Zr-Fe through measurements of superconducting properties and magnetic susceptibility. For the Zr-Cu and Zr-Ni systems, they found that  $N(E_F)$ , as determined from the rate of change of the upper critical field with temperature near the superconducting transition temperature  $T_c$ , increases approximately linearly with zirconium content. Samwer and Lohneysen<sup>7</sup> determined  $N(E_F)$  from both superconducting measurements and low-temperature specific heat for the Zr-Cu system, and also obtained an approximately linear increase with zirconium content.

We have made detailed measurements of the specific heat of liquid-quenched amorphous Ni-Zr alloys as a function of composition from 55 to 74 at. % Zr. Our determinations of  $N(E_F)$  are in approximate numerical agreement with the results of Altounian and Strom-Olsen,<sup>9</sup> but our measurements also reveal an unusual variation of  $N(E_F)$  in the composition range between 60 and 67 at. % Zr, which suggests that short-range order in the glass varies rapidly with composition in this range. The occurrence of phase separation in a few of the as-quenched specimens is conclusively demonstrated by the appearance of two superconducting transitions. A limited effort has been made to find the effects of annealing at low temperatures on these transitions. We have analyzed qualitatively these results in terms of an "association model" for liquid alloys discussed by Predel<sup>11,12</sup> and Sommer<sup>13-15</sup> according to which short-range order in the liquid is described in terms of associations or clusters of associations of specific stoichiometries in equilibrium with unassociated atoms. The concentrations of the associates vary with composition, and should be maximal for sample compositions corresponding to the stoichiometry of the associate. Thus, according to Sommer,<sup>14</sup> the favored asso-

ciate stoichiometries should be discernible from the variations with composition of structure-sensitive properties. From our measurements of the density of states at the Fermi level, superconducting transition temperatures, and the enthalpy change on crystallization, and from the resistivity measurements of Altounian and Strom-Olsen,<sup>9</sup> we have concluded that in our samples, associates with compositions of  $Zr_2Ni$  and  $Zr_3Ni_2$  tend to occur. The results are also discussed in relation to a recent paper by Moruzzi *et al.*<sup>16</sup> on the stability and electronic properties of transition-metal glasses.

## II. EXPERIMENTAL PROCEDURES

Alloy buttons of the various compositions were made by arc-melting high-purity components (Zr, 99.99% purity; Ni, 99.99% purity) in an argon atmosphere. Samples were rapidly quenched in an arc-hammer apparatus using hammer speeds of approximately 8 m/sec, resulting in (20–30)- $\mu$ m-thick foils. Average cooling rates are estimated to be in excess of  $10^6$  K/sec.<sup>17</sup> All specimens were determined to be fully amorphous to the resolution of x-ray diffraction.

Low-temperature heat capacities were measured with a small-sample calorimeter using elements of designs previously described by Råde,<sup>18</sup> and by Stewart and Giorgi.<sup>19</sup> The thermal-relaxation method was employed with an electronic system roughly similar to that described by Schwall *et al.*<sup>20</sup> The measurement is done inside a vacuum can surrounded by liquid helium. The sample holder was a 1.27-cm-diam, 0.025-cm-thick sapphire disk on which an amorphous metal heater was vapor-deposited. The gold leads of a bare germanium resistance thermometer (mass  $\sim 3$  mg) were attached to the disk and to 0.004-cm-diam manganin leads with silver-impregnated conductive epoxy. Heater leads and a 0.005-cm-diam copper wire (10–15 cm long and wound into a coil, which served as a heat link between the sample assembly and a large copper block) were similarly attached to the disk. The copper block served as a heat reservoir, the temperature of which could be controlled above the liquid-helium bath temperature by means of a heater and thermal link to the bath. Samples were stuck to the disk with weighed amounts ( $\sim 200$ – $400$   $\mu$ g) of Apiezon N grease, the heat capacity of which has been measured by others.<sup>21,22</sup> Sample masses were 10–20 mg, and sample heat capacities were generally between 50 and 80% of the total heat capacity of the sample assembly. Measurements were made from approximately 1.7 K (which is below the superconducting transition temperature  $T_c$  for all compositions) up to about 6.3 K. A 40-mg high-purity copper disk, which has a heat capacity similar to that of our specimens, was used as a standard to check operation of the system and the determination of the addendum heat capacity. Values of the intercept  $\gamma$  and the slope  $\beta$  of  $C/T$  vs  $T^2$  are always within 3% of the accepted literature values for copper.<sup>23</sup> The ( $2\sigma$ ) or 95%-confidence-level limits for the value of  $\gamma$ , as determined by the scatter in the data is about  $\pm 1\%$ .

A Perkin-Elmer differential scanning calorimeter (model DSC-II) was used to measure the enthalpy change on crystallization and to look for glass transitions in a few

specimens. Low-temperature anneals of a few specimens were done in vacuum in sealed Pyrex tubes. To minimize oxygen contamination during the anneals, specimens were wrapped in zirconium foil, and yttrium filings were placed in the bottom of the tube.

## III. RESULTS

With a few exceptions (to be discussed), plots of  $C/T$  vs  $T^2$  indicated sharp superconducting transitions (widths  $\sim 30$ – $50$  mK). All plots were linear from the superconducting transition temperature  $T_c$  up to 6.3 K, the highest temperature at which data were taken, indicating a good fit to the usual form for  $C$  at temperatures well below the Debye temperature  $\Theta_D$ ,

$$C = \gamma T + \beta T^3. \quad (1)$$

Therefore, we may relate  $\gamma$  and  $\beta$  to the density of states at the Fermi level and  $\Theta_D$  as follows:

$$N_\gamma(E_F) = 3\gamma / \pi^2 k_B^2 = (1 + \lambda) N_b(E_F), \quad \Theta_D = \left[ \frac{12\pi^4 R}{5\beta} \right]^{1/3}, \quad (2)$$

where  $k_B$  is Boltzmann's constant,  $R$  is the gas constant, and  $\lambda$  is the electron-phonon interaction parameter, which can be estimated from  $\Theta_D$  and  $T_c$  through the McMillan equation.<sup>24</sup>  $N_b(E_F)$  is the band structure, or bare density of electron states at the Fermi level, and  $N_\gamma(E_F)$ , the "specific-heat" value, is enhanced by the electron-phonon interaction.

Figure 1 shows the variation of  $N_\gamma(E_F)$  with composition from 55 to 74 at. % Zr. Also shown for purposes of comparison are values of  $N_\gamma(E_F)$  obtained by Altounian and Strom-Olsen<sup>9</sup> from measurements of the superconducting transition temperature  $T_c$ , the slope of the upper critical field,  $H_{c2}$ , as a function of temperature near  $T_c$ , and the normal-state resistivity at low temperature. Differences between the two measurements are striking,

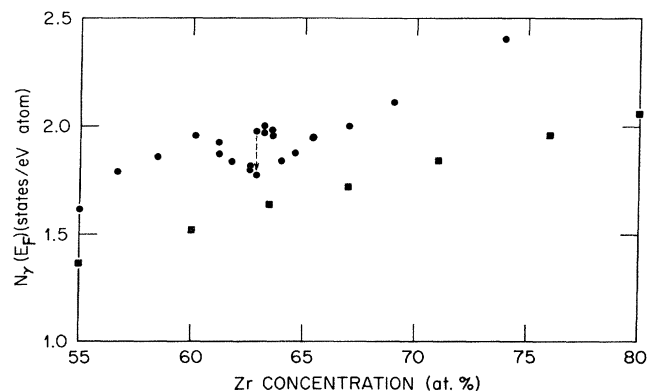


FIG. 1. Density of states at the Fermi level,  $N_\gamma(E_F)$ , as a function of zirconium content. Circles are the present work and the squares are from Ref. 9. Arrow shows the change in  $N_\gamma(E_F)$  for a 62.9-at. % Zr specimen when it was annealed for 30 min at  $150^\circ\text{C}$ .

but it should be noted that for both sets of data the general trend is for  $N_\gamma(E_F)$  to increase with zirconium content, as expected. The values from  $H_{c_2}(T)$  are approximately 10–20% lower than those obtained from specific heat. A similar difference was found for glassy Cu-Zr alloys by Samwer and Lohneisen,<sup>7</sup> who determined  $N_\gamma(E_F)$  by both methods. An interesting aspect of the data is the rapid variation of  $N_\gamma(E_F)$  with composition between 60 and 65 at. % Zr. It is reasonable to interpret this “structure” as indicating that the short-range order changes abruptly with composition.

It is interesting to discuss possible reasons why the data of Altounian and Strom-Olsen show no indication of this unusual variation of  $N_\gamma(E_F)$ . First, it should be noted that over the range of our data, 55–74 at. % Zr, Altounian and Strom-Olsen have only five points, and these are spaced such that the rapid variations of our  $N_\gamma(E_F)$  values might appear only as rather large scatter on their data. However, their points fit closely on a straight line, and it is probable that the difference between the two measurements is not merely apparent, but real. In this case, the difference must be due either to differences between specimens, or to the fact that  $N_\gamma(E_F)$  was derived in the two cases from measurements of different physical quantities. Altounian and Strom-Olsen used melt-spun ribbons, whereas our specimens were quenched by arc hammer, so that the difference could result from different cooling curves during glass formation. However, our results indicate that thermal relaxation of Ni-Zr glasses results in a lowering of the superconducting transition temperature, and our  $T_c$ 's agree rather well with those of Altounian and Strom-Olsen, suggesting that cooling-rate differences are not important. Onn *et al.*<sup>8</sup> measured the specific heat for three samples in this composition range, also made by melt-spinning. Their  $T_c$ 's were 0.25–0.3 K lower than ours and those in Ref. 9, suggesting that quench rates in this case were lower. We have also found that oxygen contamination tends to lower  $T_c$ . Their  $N_\gamma(E_F)$  values were, in one case, intermediate between ours and Ref. 9, and in two cases essentially the same as in Ref. 9.

Another possibility is that the difference between the two results arises from the fact that heat capacity is a bulk property, and the value of  $\gamma$  derived from our measurements is a characteristic of the whole specimen, whereas a resistively measured  $H_{c_2}$  may, in an inhomogeneous or phase-separated material, be characteristic only of the higher  $H_{c_2}$  phase, provided this phase has sufficient connectivity to carry current. Thus, phase separation could account for some differences between the two measurements. As we shall see, we do have evidence, in the form of two superconducting transitions, of phase separation for some compositions. However, the 10–20% differences in magnitude of  $N_\gamma(E_F)$  for compositions where we do not find evidence of separate phases must have another reason. Aside from the previously mentioned difference between specific-heat- and  $H_{c_2}(T)$ -derived values of  $N_\gamma(E_F)$  for Cu-Zr glasses<sup>7</sup> (which the authors speculate is due to uncertainties in their resistivity measurements), most comparisons of the two within measurements (in both amorphous and crystalline materials) have agreed

within experimental error.<sup>25,26</sup>

The 62.9-at. % Zr composition lies at the low zirconium edge of the plateau in  $N_\gamma(E_F)$  (Fig. 1), and was unique among our as-quenched specimens in that its  $C(T)$  curve shows evidence of the presence of two superconducting phases of comparable volume fractions. For one other composition, 56.7 at. % Zr, evidence of a small amount of a second phase is seen. Figure 2(a) shows  $C/T$  vs  $T^2$  for the 62.9-at. % Zr alloy in the as-quenched condition. As with all of the specimens, the plot is linear above the superconducting transition. The value of  $\gamma$  places  $N_\gamma(E_F)$  on the plateau, equal to  $N_\gamma(E_F)$  for the 63.2 and 63.6-at. % Zr specimens. The superconducting transition was observed to be wider than usual, and a closer examination of the transition region is shown in Fig. 2(c), which we interpret as indicating two superconducting transitions. Two points shall be discussed about this interpretation. First, we are limited in how small a difference in  $T_c$  we can resolve by our measurement technique. In the relaxation-time-constant method which we employed, a temperature difference  $\Delta T$  is established between the sample assembly and a copper block by means of an electric heater on the sample holder. Then, the heater current is switched off, and the time constant for decay of the temperature of the sample assembly to the temperature of the copper block is measured. The heat capacity thus measured is an average over the temperature interval covered by  $\Delta T$ . We cannot resolve structure in  $C(T)$  which has a width on the order of or smaller than the value of  $\Delta T$ . We normally use  $\Delta T$  between 30 and 60 mK, but for examining the transition region, we found we could use  $\Delta T$  as small as 10–15 mK without introducing large scatter in the data. The practical lower limit on  $\Delta T$  is determined by amplifier noise in the circuit used to measure the temperature as a function of time during decay. Thus, features in  $C(T)$ , which are on the order of 15 mK or smaller, cannot be accurately defined. The transition for the as-quenched 62.9-at. % Zr alloy is approximately 150 mK wide. Second, for a specimen consisting of two superconducting phases with different  $T_c$ 's to exhibit two distinct superconducting transitions, the dimensions of the phases must be at least as large as the superconducting coherence length  $\xi(T=0)$  for the separate phases.<sup>27</sup> For Zr-Ni glasses,  $\xi(0) \sim 60 \text{ \AA}$ , and is presumably not very different for the two phases. We regard the data of Fig. 2(c) as clear evidence of two superconducting phases. The first, or lower- $T_c$ , decrease in heat capacity is smaller than the second one, indicating that the lower- $T_c$  phase is the minor phase, but it nevertheless occupies a significant portion of the specimen.

The 62.9-at. % Zr specimen was annealed for 30 min at 150°C ( $T_x \sim 400^\circ\text{C}$ ), and its heat capacity was measured again. Figure 2(b) shows  $C/T$  vs  $T^2$ , and Fig. 2(c) shows details of the superconducting transition. After this short, low-temperature anneal, the value of  $N_\gamma(E_F)$  was lower and in line with the values for lower zirconium compositions (see arrow, Fig. 1). The sample still has two superconducting transitions, but the volume fraction of the higher- $T_c$  phase has apparently decreased greatly. In Fig. 2(c) the solid lines through data points above the transitions for each curve are the least-squares fit of all the data

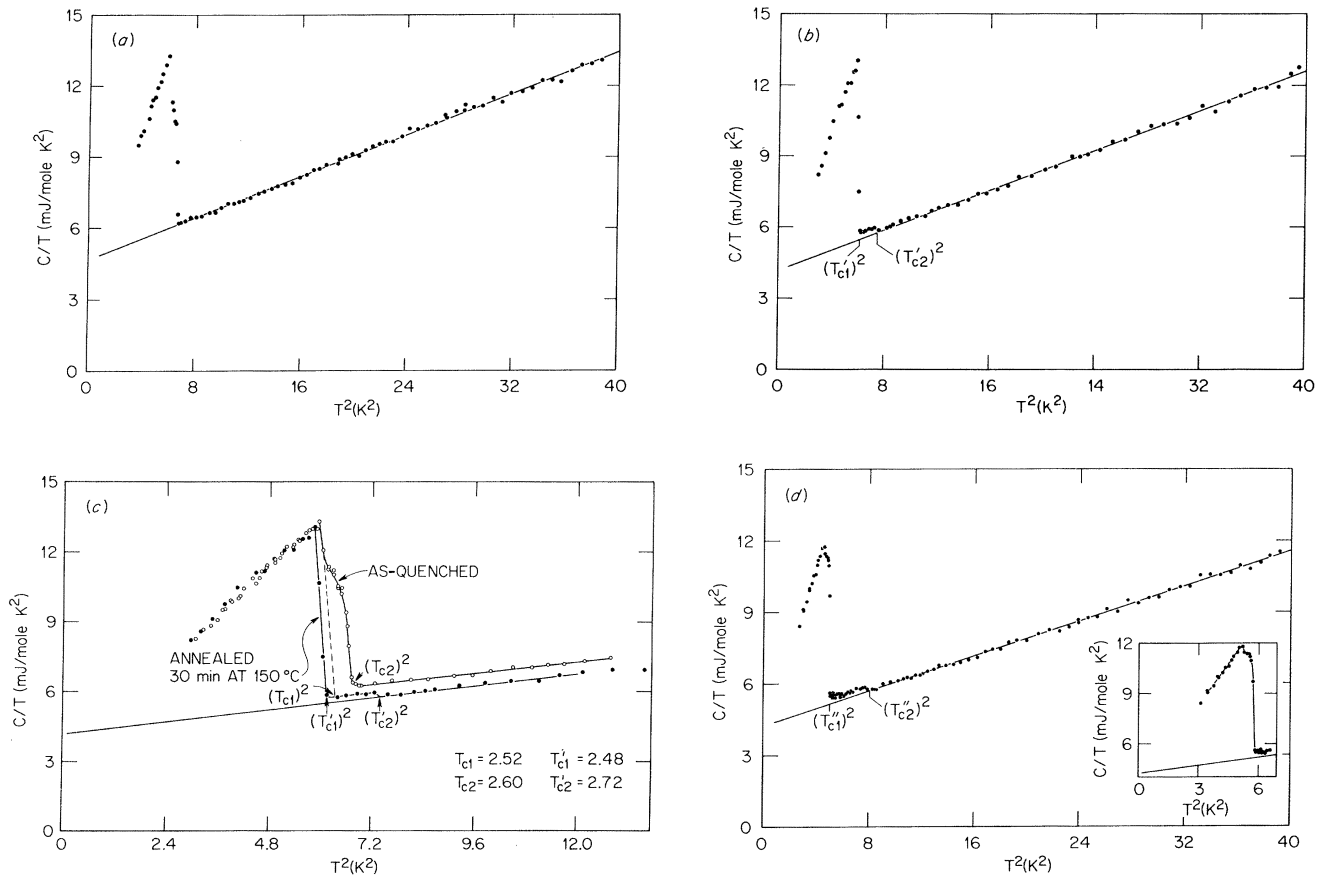


FIG. 2. (a)  $C/T$  vs  $T^2$  for the 62.9-at. % Zr as-quenched specimen. The step at the superconducting transition is broader than usual, and its shape suggests the occurrence of two transitions [see Fig. 2(c)]. Above the transition the plot is linear, as it was in all of the specimens. (b)  $C/T$  vs  $T^2$  for the 62.9-at. % Zr specimen after annealing for 30 min at 150°C. The main transition is sharp, and apparently corresponds to the lower- $T_c$  transition in the as-quenched condition. The high- $T_c$  transition at  $T'_{c2}$  now involves a small fraction of the sample. (c) Expanded view of the transitions for the 62.9-at. % Zr specimen as-quenched and annealed for 30 min at 150°C. In the as-quenched condition the transition clearly involves two steps, implying the presence of two superconducting phases.  $T_{c1}$  and  $T_{c2}$  identify the temperatures at which those phases have completely transformed to the normal state. After annealing, the step at the higher-temperature transition at  $T'_{c2}$  is small, indicating that only a small portion of the specimen is involved. The lines are least-squares fits to all of the data above the transition region. (d)  $C/T$  vs  $T^2$  for the 62.9-at. % Zr specimen after annealing for 20 h at 275°C. The high-temperature tail now extends to  $T''_{c2} = 2.83$  K, and the step at  $T''_{c2}$  remains small. The main transition was broadened by this anneal and the shape (see inset) now suggests the presence of a third phase.

from the transition to  $T^2 = 40$ . The tail lying above this line, which remains after the sharp main transition has occurred, indicates that a small fraction of the specimen remains superconducting up to  $T = T'_{c2}$ . The increase in  $T_c$  of the higher  $T_c$  phase is presumably a result of coarsening of the phases, with a consequent lessening of the proximity effect. The lower  $T_c$  transition moved downward slightly. The decrease in volume fraction of the higher- $T_c$  phase upon annealing suggests that this phase is more stable near the melting point than at the annealing temperature. The low  $T_c$  changed very little during the anneal, which suggests that the low- $T_c$  regions in the as-quenched condition were sufficiently large so that their  $T_c$  was not strongly affected by proximity to the higher- $T_c$  phase. It should be stated that identification of

the higher- $T_c$  phase after annealing with the one present before annealing is an assumption for which we have no corroborating evidence.

An additional anneal was performed on the 62.9-at. % Zr specimen for 20 h at 275°C. The apparent volume fraction of the high- $T_c$  phase did not change significantly, as can be seen from the height of the tail in Fig. 2(d), but both of the  $T_c$ 's changed. The  $T_c$ 's are all indicated on the plot of  $T_c$  vs Zr content in Fig. 3.  $N_\gamma(E_F)$  was essentially unchanged by this additional anneal. The peak in  $C/T$  vs  $T^2$  at the superconducting transition is not sharp, but rounded and rather broad, in contrast to the curve after 30 min at 150°C, and to the transitions seen in most of the as-quenched specimens. It is usual for anneals at temperatures below crystallization to result in sharper su-

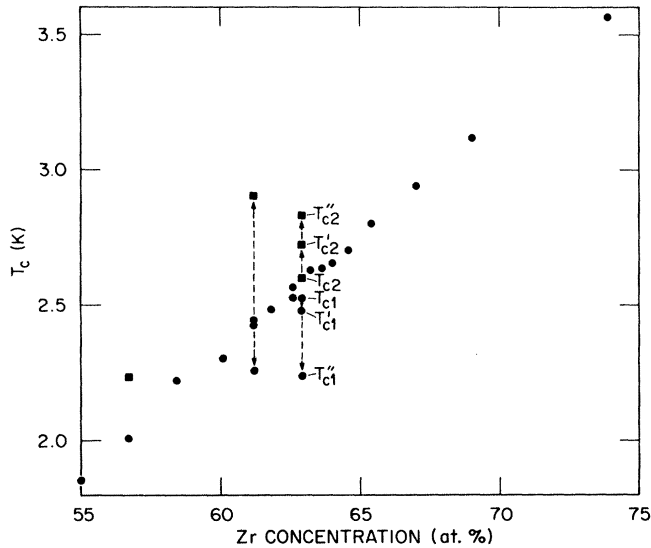


FIG. 3. Superconducting transition temperatures  $T_c$  as a function of zirconium content. For samples showing two transitions the higher  $T_c$  is indicated by a square. Arrows indicate changes caused by annealing. For the 61.2- and 62.9-at. % Zr compositions, annealing resulted in lower transitions with  $T_c$ 's similar to the value at 60 at. % Zr, and higher transitions with  $T_c$ 's similar to the value at 66.7 at. % Zr (interpolated value = 2.92 K). The labeled  $T_c$ 's for 62.9 at. % Zr correspond to transitions identified in Fig. 2. The 56.7-at. % Zr specimen as quenched showed two transitions, the upper one having a  $T_c$  similar to the value at 60 at. % Zr.

perconducting transitions, presumably because structural relaxation leads to a more homogeneous structure with fewer long-range defects or strain fields.<sup>28</sup> A careful, long-time x-ray-diffraction examination of the specimen revealed no evidence of crystallinity. Structure within the transition [see inset, Fig. 2(d)] suggests that there are now two phases with very similar  $T_c$ 's making up the bulk of the sample. We cannot say from superconducting  $T_c$  measurements whether annealing has created a new phase, or whether coarsening of phases already present has made them distinguishable in their superconducting properties.

DSC traces (Fig. 4) for the 62.9-at. % Zr alloy annealed for 20 h at 275°C indicate two glass transitions separated by a small exotherm. The as-quenched alloy shows one endotherm, indicating a glass transition, just before crystallization. The annealed material shows two endotherms and an exotherm of comparable size. At 80-K/min scan rate, the small exotherm and the first crystallization peak nearly obscure the second endotherm. At 160 K/min the exotherm lies between the two endotherms and at 320 K/min the exotherm is nearly obscured by the first endotherm. It is unclear whether these results indicate the presence of two endotherms separated by an exotherm or a single broad endotherm interrupted by an exotherm. These curves are similar to DSC results presented by Predel for  $\text{Ni}_{34}\text{Pd}_{48}\text{P}_{18}$  glass.<sup>11</sup> Predel identified the small exotherm with the process of phase separation. The changes in DSC traces brought about by the 20 h at 275°C

anneal suggest that the anneal resulted in an amorphous phase which was not present as-quenched. This interpretation is consistent with the low-temperature specific-heat result.

Further evidence of phase separation was found in the heat-capacity measurements of an as-quenched specimen at 56.7-at. % Zr and in a 61.2-at. % Zr sample which had been annealed. The 56.7-at. % Zr sample had a narrow transition for most of the sample at 2.01 K, and a high- $T_c$  tail, which extended to 2.24 K. Two 61.2-at. % Zr samples were run, neither of which showed evidence of phase separation as quenched. One of them was annealed for 1 h at 200°C, after which the  $C/T$ -vs- $T^2$  plot showed a narrow transition for the bulk of the material at 2.26 K (down from 2.44 K as-quenched) and a high- $T_c$  tail extending up to about 2.9 K. Table I shows values of the various properties, which can be derived from the heat-capacity measurements at low temperatures.

A study of the crystallization process by DSC is in progress and will be published soon.<sup>29</sup> One experimental result from this study is especially pertinent to the interpretation of the present results from low-temperature specific heat. Figure 5 shows the enthalpy change  $\Delta H$  on crystallization as a function of composition. Above approximately 65 at. % Zr,  $\Delta H$  is essentially independent of composition except for a shallow minimum at the eutectic at 75.9 at. % Zr. The most interesting feature is a deep minimum

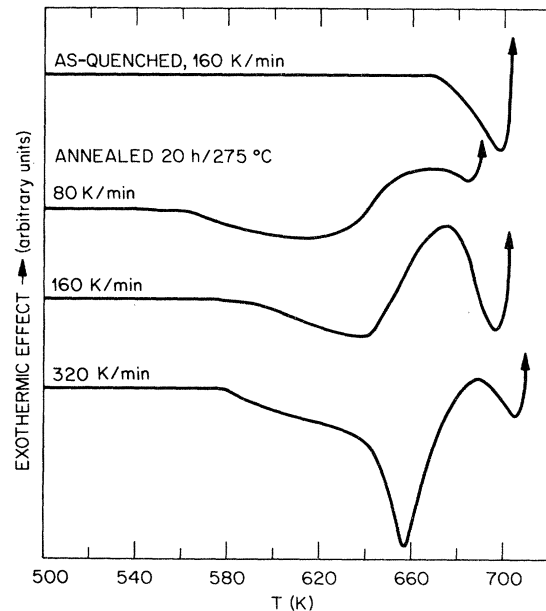


FIG. 4. DSC traces for 62.9-at. % Zr alloy. As-quenched, there is a single endotherm prior to crystallization. The corresponding specific-heat curve indicates two major phases, but as we see in Figs. 2(b) and 2(c), annealing at low temperature rapidly reduces the volume fraction of one phase. After annealing for 20 h at 275°C, two endotherms separated by an exotherm are evident. The specific heat for this condition is shown in Fig. 2(d).

TABLE I. Quantities derived from specific-heat measurements. Superscripts a and b distinguish different samples of the same composition.

Zr content (at. %)	$N_{\gamma}(E_F)$ (states/eV atom)	$\Theta_D$ (K)	$T_{c_1}$ (K)	$T_{c_2}$	Condition	$\lambda$ ( $\mu^* = 0.14$ )
55	1.61	220	1.85		as-quenched	0.555
56.7	1.79	215	2.01	2.24	as-quenched	0.569
58.4	1.86	212	2.22		as-quenched	0.584
60.1	1.96	207	2.30		as-quenched	0.593
61.2 <sup>a</sup>	1.92	207	2.44		as-quenched	0.602
61.2 <sup>a</sup>	1.91	212	2.26	2.90	1 h at 200°C	0.587
61.2 <sup>b</sup>	1.87	203	2.42		as-quenched	0.603
61.8	1.84	204	2.49		as-quenched	0.607
62.6 <sup>a</sup>	1.82	206	2.52		as-quenched	0.607
62.6 <sup>b</sup>	1.80	203	2.57		as-quenched	0.613
62.9	1.98	207	2.52	2.60	as-quenched	0.607
62.9	1.78	210	2.48	2.72	30 min at 150°C	0.602
62.9	1.79	219	2.24	2.83	20 h at 275°C	0.581
63.2 <sup>a</sup>	2.00	194	2.63		as-quenched	0.624
63.2 <sup>b</sup>	1.98	199			as-quenched	
63.6 <sup>a</sup>	1.99	199	2.64		as-quenched	0.621
63.6 <sup>b</sup>	1.96	201			as-quenched	
64	1.84	201	2.65		as-quenched	0.620
64.6	1.88	198	2.70		as-quenched	0.625
65.4	1.95	198	2.80		as-quenched	0.631
67	2.01	194	2.94		as-quenched	0.644
69	2.12	191	3.12		as-quenched	0.658
73.9	2.40	189	3.56		as-quenched	0.687

at 58–59 at. % Zr, a composition at which the equilibrium phase diagram shows no feature.

#### IV. DISCUSSION

These results will be discussed in relation to ideas presented by Predel<sup>11,12</sup> and Sommer<sup>13–15</sup> on the importance of “atomic associations,” i.e., short-range order to the process of glass formation. According to Sommer’s association model for liquid alloys,<sup>13,14</sup> alloy melts with compound-forming tendencies contain associates, or clusters of associates of unlike atoms, which are in dynamic equilibrium with the unassociated atoms. This equilibrium is governed by the mass-action law, so that the volume fraction and stoichiometric composition of the ordered re-

gions are functions of temperature. Stoichiometric compositions of the ordered regions are limited to simple whole-number ratios of the constituents, such as  $A_2B$ ,  $A_3B_2$ ,  $AB$ , etc. The spatial extent of the associate clusters remains undefined. It is Sommer’s thesis that glass-forming tendency is enhanced by the occurrence of such associates provided that their stoichiometry is different from that of nearby equilibrium crystalline phases. Not only do the associations tend to reduce the free-energy difference between the liquid and crystalline states, but the presence of associations with a different stoichiometry from nearby equilibrium crystalline phases tends to slow the kinetics of crystal-nucleus formation.

The concentration of associated atoms varies with composition and is a maximum when the overall composition matches that of the associates. Therefore, structure-sensitive properties are likely to exhibit peculiarities in their concentration dependences near these concentrations. Assuming that the structure of the liquid is preserved in the glass (as has been demonstrated by Sakata *et al.*<sup>30</sup> for CuTi glasses), property variations in the glass can be used to identify the compositions of the associates. The superconducting transition temperature and the density of states at the Fermi level as determined from low-temperature specific-heat measurements, as well as the enthalpy change on crystallization  $\Delta H$  have been used here for this purpose.

Consider first the enthalpy change upon crystallization  $\Delta H$  shown in Fig. 5. The changes in free energy and entropy upon crystallization both contribute to  $\Delta H$ . Since the crystallized specimens in this composition range con-

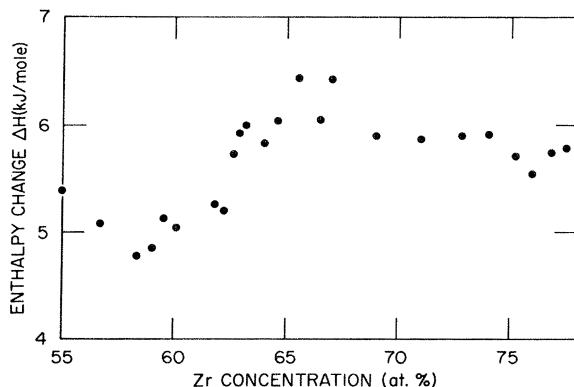


FIG. 5. Enthalpy change on crystallization  $\Delta H$  as a function of zirconium content.

sist of a mixture of  $Zr_2Ni$  and  $ZrNi$  phases, the free energy and entropy of the crystalline state should vary slowly with composition. Therefore, the minimum in  $\Delta H$  at 58–59 at. % Zr indicates a strong reduction of the free energy and/or entropy of the supercooled liquid just above the glass transition temperature  $T_g$ , from which crystallization takes place. We expect the free energy and the entropy both to be reduced by associate formation, and interpret the  $\Delta H$  variation as suggesting the presence of  $Zr_3Ni_2$ -type associates. The slight displacement of the minimum from 60 at. % Zr is probably a consequence of the combined variations of entropy and free energy in the liquid and crystalline states.

conducting transition in their specific-heat curves also provide information about stoichiometry of the associates. In most cases the transitions were sharp, indicating that any compositional clusters present are so small that the proximity effect prevents them from being seen as separate transitions. In those cases where separate transitions are seen, dimensions of the clusters must be at least on the order of the superconducting coherence length  $\xi(T=0)$ , which for these alloys is approximately 60 Å. The proximity effect and the decrease of  $T_c$  with structural relaxation are complicating factors in the identification of phases from their  $T_c$ 's. Nevertheless, the evidence in Fig. 3 points toward both  $Zr_3Ni_2$  and  $Zr_2Ni$  associates. The  $T_c$  for as-quenched 66.7-at. % Zr glass, as can be seen from Fig. 3, is 2.9 K, and the  $T_c$  for as-quenched 60-at. % Zr glass is 2.3 K. After the 62.9-at. % Zr specimen was annealed for 20 h at 275°C, it had transitions at 2.83 and 2.24 K, and the 61.2-at. % Zr specimen, after annealing for 1 h at 200°C, had transitions at 2.9 and 2.26 K. These results point to a high- $T_c$  phase with  $T_c \sim 2.8$ –2.9 K and a low- $T_c$  phase with  $T_c$  about 2.25 K, values which are close to but somewhat lower than the  $T_c$ 's for as-quenched  $Zr_2Ni$  and  $Zr_3Ni_2$  glasses. The 56.7-at. % Zr specimen, as quenched, also exhibited a small high- $T_c$  tail extending to 2.24 K, while the main superconducting transition was sharp and occurred at 2.01 K. We may suppose from this result that the majority of that sample consists of unassociated atoms or unassociated atoms along with clusters too small to have distinguishable superconducting properties, and that the high- $T_c$  tail results from a small percentage of large  $Zr_3Ni_2$  clusters. The possible third phase with a  $T_c$  less than 2.24 K indicated by breadth and structure in the superconducting transition of the annealed 62.9-at. % Zr sample [see inset, Fig. 2(d)] may also be due to unassociated atoms.

Further evidence that the 60-at. % Zr and 66.7-at. % Zr compositions are special is seen in the electrical resistivity measurements of Altounian and Strom-Olsen<sup>9</sup> plotted in Fig. 6. The variation from 30 to 60 at. % Zr is smooth, but peculiarities are evident near both 60 and 66.7 at. % Zr.

Assuming that we have correctly concluded that clusters of compositions  $Zr_3Ni_2$  and  $Zr_2Ni$  both tend to occur in the composition range studied, we can speculate as follows about the variations of  $N_\gamma(E_F)$  and of the concentrations of clusters with composition. The concentration of an associate is expected to be maximal for the composition corresponding to the associate stoichiometry. Thus, as

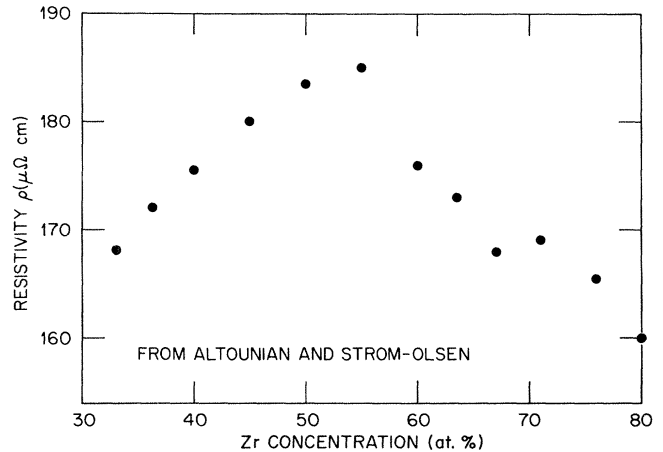


FIG. 6. Electrical resistivity  $\rho$  as a function of zirconium content for melt-spun Zr-Ni ribbons (from Ref. 9).

zirconium content decreases from 66.7 at. % Zr, the concentration of  $Zr_2Ni$  associates decreases. If  $Zr_3Ni_2$  associates are present near 66.7 at. % Zr, their concentration should increase as zirconium content decreases. At approximately 64 at. % Zr, the concentrations of both types of associates apparently increase sharply, since  $N_\gamma(E_F)$  abruptly increases to the value at 60 and 66.7 at. % Zr (these happen to be the same). We may speculate that in the approximately 1-at. %-composition interval of the  $N_\gamma(E_F)$  plateau, the concentration of unassociated atoms is relatively low. The specific-heat curve for the as-quenched 62.9-at. % Zr specimen indicates that the higher- $T_c$  transition, which we identify with  $Zr_2Ni$  associates, involves around one-half of the specimen. The plateau lies halfway between 60 and 66.7 at. % Zr, so that if half the specimen has one composition, the remainder must have the other composition. On this basis, we speculate that on the plateau, the specimens have low concentrations of unassociated atoms. At 62.6 at. % Zr, the concentration of  $Zr_2Ni$  clusters in the as-quenched sample decreases abruptly, and  $N_\gamma(E_F)$  is characteristic of a mixture of  $Zr_3Ni_2$  clusters and unassociated atoms. As the zirconium content approaches 60 at. % Zr the concentration of  $Zr_3Ni_2$  clusters increases, and  $N_\gamma(E_F)$  increases to a maximum at about 60 at. % Zr. It is interesting to note that the equilibrium phase diagram shows a eutectic at 63.5 at. % Zr, just halfway between the compositions corresponding to the two types of associates we infer to be present, and coinciding with the  $N_\gamma(E_F)$  plateau.

Although we find that most of our observations are consistent with the above interpretation, there are some points which remain confusing. For instance, annealing the 62.9-at. % Zr sample at a low temperature apparently resulted in a decreased concentration of associates. The tendency to form associates is expected to increase with decreasing temperature. It is also unexpected that such a short-time, low-temperature anneal (30 min at 150°C) should result in a drastic change in the apparent fraction of the specimen with higher  $T_c$ . As evidence counter to our interpretation we might also mention that the partial radial distribution functions determined by Wagner and Lee<sup>31</sup> for  $Zr_{65}Ni_{35}$  glass indicate a weak preference for un-

like neighbors in the first coordination shell. This result appears to be inconsistent with the presence of associates of unlike atoms. We make two comments. First, at 65 at. % Zr, the variation of  $N_V(E_F)$  suggests that the concentration of associates is indeed small. Second, there is reason to question the applicability of these partial distribution functions to our specimens. Wagner and Lee<sup>31</sup> used Hf in an isomorphous substitution for zirconium in a series of  $\text{Ni}_{35}(\text{Zr-Hf})_{65}$  alloys. Zirconium and hafnium have similar atomic radii and the intermediate crystalline phases in the two systems Zr-Ni and Hf-Ni are isostructural, but the eutectic between ZrNi and  $\text{Zr}_2\text{Ni}$  occurs at 63.5 at. % Zr and the eutectic between Hf-Ni and  $\text{Hf}_2\text{Ni}$  is at 62 at. % Hf. Since the effects which we observe are a sensitive function of composition in this range, the consequence of substituting hafnium for zirconium is unknown.

Much of what is known about crystallization and glass-forming tendency of Zr-Ni in this composition range is consistent with the presence of  $\text{Zr}_3\text{Ni}_2$  and  $\text{Zr}_2\text{Ni}$  associates. In the composition interval from 60 to 66 at. % Zr, Dong *et al.*<sup>32</sup> and Buschow *et al.*<sup>33</sup> found that DSC traces show two crystallization peaks, the relative heights of which vary with composition. In some cases, a third exotherm was observed. Dong *et al.*<sup>32</sup> found, from x-ray-diffraction patterns taken from specimens heated to various temperatures within the crystallization range, that the first DSC peak for a 62-at. % Zr alloy involved crystallization of  $\text{Zr}_2\text{Ni}$ , and the second crystallization of the compound ZrNi from the nickel-enriched glass. We have similarly concluded for 63.6 at. % Zr that the first peak involves crystallization of  $\text{Zr}_2\text{Ni}$ . Also, Scott *et al.*<sup>34</sup> found that the first crystalline phase to appear during isothermal crystallization of 63.5-at. % Zr glass is  $\text{Zr}_2\text{Ni}$ , and we have determined that for 60-at. % Zr alloy the first crystalline phase to appear is ZrNi. We conclude that for zirconium content greater than 62 at. % Zr the first DSC peak involves crystallization of  $\text{Zr}_2\text{Ni}$ , and that between 60 and 62 at. % Zr, the character of the first peak changes. For zirconium content less than 60 at. % Zr, only one DSC peak occurs, during which both ZrNi and  $\text{Zr}_2\text{Ni}$  crystallize. We interpret these results to indicate that the presence of  $\text{Zr}_2\text{Ni}$  associates in the glass (more importantly in the supercooled liquid just above  $T_g$ ) promotes crystallization of the compound  $\text{Zr}_2\text{Ni}$ . As the zirconium content decreases to 60 at. % Zr the concentration of  $\text{Zr}_2\text{Ni}$  associates decreases, and crystallization of  $\text{Zr}_2\text{Ni}$  is no longer favored. For zirconium content greater than 62 at. % Zr, crystallization of ZrNi is apparently impeded by the presence of  $\text{Zr}_3\text{Ni}_2$  associates, since ZrNi crystallizes in a second DSC peak only after the composition of the supercooled liquid has been altered by crystallization of  $\text{Zr}_2\text{Ni}$ . A more complete discussion of the effect of these associates on the crystallization process has been published elsewhere.<sup>29</sup>

We do not know in detail how glass-forming ability varies as a function of composition in the Zr-Ni system. We believe from our experience at making splats, that glass formation is easier near the eutectic at 63.5 at. % Zr than near either 60 or 66.7 at. % Zr. The only effort to obtain quantitative estimates of critical cooling rates for

glass formation in this system was made by Nishi *et al.*<sup>35</sup> who found that the cooling rate required to produce partially amorphous specimens is reduced in the range from 60 to 70 at. % Zr, but they found no minimum in this composition range in the cooling rate required to make fully amorphous samples. This result is consistent with the presence of  $\text{Zr}_2\text{Ni}$  associates in the melt, since they would promote the formation of  $\text{Zr}_2\text{Ni}$  crystal nuclei.

Moruzzi *et al.*<sup>16</sup> recently presented a discussion of the relationship between the electronic properties and stability of transition-metal glasses. They present evidence that the density of electron states for the glass is similar in those aspects determined by short-range interatomic interactions to that of highly coordinated close-packed structures (e.g., fcc), which the alloy might assume on crystallization. They argue that glass formation is more probable for alloy systems and compositions at which these close-packed crystal structures have a high energy, and are therefore less stable. Because of the similarity between the density of states of the glass and that of the corresponding close-packed crystal structure, they argue that the liquid at glass-forming compositions also has a high energy and therefore is also relatively unstable. Basic to their argument is an observed correlation between the density of states at the Fermi level and the total energy, so that a high  $N(E_F)$  implies a high-energy, less-stable configuration. Thus, they anticipate that at easy glass-forming compositions the glass will have a relatively high  $N(E_F)$ . Moruzzi *et al.*<sup>16</sup> point out that this conclusion is essentially opposite to the Nagel-Tauc model,<sup>36</sup> from which one expects stable liquids with low  $N(E_F)$  at easy glass-forming compositions.

Surprisingly, the variation of  $N(E_F)$  near the eutectic at 63.5 at. % Zr could be interpreted to provide support for either of these views. There is a tendency toward a minimum in  $N(E_F)$ , but for reasons not understood, in the immediate vicinity of the eutectic there apparently is a sharp increase in the concentration of associates of both types, resulting in the  $N(E_F)$  plateau. Moruzzi *et al.*<sup>16</sup> suggest that the liquid may support small, local stoichiometry fluctuations and that these may promote glass formation. Perhaps these stoichiometry fluctuations should be identified with associate formation and clustering. There is an alternative, and perhaps a more appropriate interpretation of the  $N(E_F)$  dependence which does not involve a minimum at the eutectic. The  $N(E_F)$  plateau and the maximum at 60 at. % Zr may be viewed as positive deviations from the expected general decrease in  $N(E_F)$  with increasing nickel content. The data then appear to be in general agreement with the ideas presented by Moruzzi *et al.*<sup>16</sup> The maximum at 60 at. % Zr would result from the liquid assuming short-range order characteristic of a high-energy crystal structure, which is unstable since it is not present in the equilibrium phase diagram. This structure would of course have the stoichiometry of  $\text{Zr}_3\text{Ni}_2$  associates.  $N(E_F)$  for the glass is not elevated near 66.7 at. % Zr. The  $\text{Zr}_2\text{Ni}$  associates, which we expect to have maximum concentration at this composition, may have near-neighbor coordination similar to the equilibrium  $\text{Zr}_2\text{Ni}$  intermetallic compound, which has a tetragonal structure (C16,  $\text{CuAl}_2$  type) with an aver-

age coordination number of  $13\frac{1}{3}$ .<sup>37</sup>

## V. CONCLUSIONS

Low-temperature specific-heat measurements of Zr-Ni glasses with compositions ranging from 55 to 74 at. % Zr reveal an unusual variation of the density of states at the Fermi level for compositions between 60 and 67 at. % Zr. Also, for a few compositions in the as-quenched condition, the temperature variation of heat capacity indicates two superconducting transitions, providing clear evidence of phase separation. By comparing the transition temperatures of the individual phases in both as-quenched and annealed samples exhibiting phase separation to a plot of  $T_c$  versus composition for all of the samples, we could identify the individual phases as having compositions near 60 and 66.7 at. % Zr. A minimum in the enthalpy change on crystallization near 60 at. % Zr, and peculiarities in the variation of electrical resistivity at 60 and 67 at. % Zr (from Ref. 9), confirmed identification of these compositions as special. These results have been discussed in terms of Sommer's association model for liquid alloys, according to which the liquid contains associations or clusters of atoms with definite stoichiometries, in equilibrium with unassociated atoms. Our results indicate that in the

composition range studied, both  $Zr_3Ni_2$  and  $Zr_2Ni$  clusters occur. The most unusual feature of the  $N_\gamma(E_F)$  variation, a sharp maximum or plateau in the interval from 62.9 to about 64 at. % Zr, is thought to result from sharply increased concentration of both  $Zr_3Ni_2$  and  $Zr_2Ni$  clusters in those samples. For other compositions it appears likely that samples contain primarily one type of cluster, with a small concentration of clusters of the other type.  $N_\gamma(E_F)$  has a maximum near 60 at. % Zr, coinciding with an expected maximum concentration of  $Zr_3Ni_2$  clusters. We find this interpretation to be consistent with recent work on crystallization and glass-forming tendency in the Zr-Ni system. The variation of  $N(E_F)$  with concentration appears to be consistent with a recent discussion by Moruzzi *et al.*<sup>16</sup> of electronic properties and stability of transition-metal-transition-metal glasses.

## ACKNOWLEDGMENTS

The authors wish to thank D. M. Nicholson and W. A. Coghlan for helpful discussions and careful review of the manuscript. We thank O. B. Cavin for x-ray-diffraction measurements. This research was sponsored by the Division of Materials Sciences, U. S. Department of Energy, under Contract No. W-7405-eng-26 with the Union Carbide Corporation.

\*Present address: Materials Engineering Department, North Carolina State University, Raleigh, NC 27650.

<sup>1</sup>P. Oelhafen, E. Hauser, H.-J. Güntherodt, and K. H. Bennemann, *Phys. Rev. Lett.* **43**, 1134 (1979).

<sup>2</sup>A. Amamou, *Solid State Commun.* **33**, 1029 (1980).

<sup>3</sup>P. Oelhafen, E. Hauser, and H.-J. Güntherodt, *Solid State Commun.* **35**, 1017 (1980).

<sup>4</sup>P. Oelhafen, R. Lapka, U. Gubler, J. Krieg, A. DasGupta, H.-J. Güntherodt, T. Mizoguchi, C. Hague, J. Kübler, and S. R. Nagel, in *Proceedings of the Fourth International Conference on Rapidly Quenched Metals, 1981, Sendai, Japan*, edited by T. Masumoto, and K. Suzuki (Institute of Metals, Sendai, Japan, 1981), Vol. II, p. 1259.

<sup>5</sup>A. DasGupta, P. Oelhafen, U. Gubler, R. Lapka, H.-J. Güntherodt, V. L. Moruzzi, and A. R. Williams, *Phys. Rev. B* **25**, 2160 (1982).

<sup>6</sup>J. Kübler, K. H. Bennemann, R. Lapka, F. Rösel, P. Oelhafen, and H.-J. Güntherodt, *Phys. Rev. B* **23**, 5176 (1981).

<sup>7</sup>K. Samwer and H. von Lohneysen, *Phys. Rev. B* **26**, 107 (1982).

<sup>8</sup>D. G. Onn, L. Q. Wang, Y. Obi, and K. Fukamichi, *Solid State Commun.* **46**, 37 (1983).

<sup>9</sup>Z. Altounian and J. O. Strom-Olsen, *Phys. Rev. B* **27**, 4149 (1983).

<sup>10</sup>F. P. Missell, S. Frota-Pessoa, J. Wood, J. Tyler, and J. E. Keem, *Phys. Rev. B* **27**, 1596 (1983).

<sup>11</sup>B. Predel, *Physica (Utrecht)* **103B**, 113 (1981).

<sup>12</sup>B. Predel, in *Calculations of Phase Diagrams and Thermochemistry of Alloy Phases*, edited by Y. A. Chang and J. F. Smith (American Institute of Metallurgical Engineers, Warrendale, Pennsylvania, 1979), p. 72.

<sup>13</sup>F. Sommer, *Z. Metallkd.* **73**, 72 (1982).

<sup>14</sup>F. Sommer, *Z. Metallkd.* **73**, 77 (1982).

<sup>15</sup>F. Sommer, K. H. Klappert, I. Arpshofen, and B. Predel, *Z. Metallkd.* **73**, 581 (1982).

<sup>16</sup>V. L. Moruzzi, P. Oelhafen, and A. R. Williams, *Phys. Rev. B*

**27**, 7194 (1983).

<sup>17</sup>D. M. Kroeger, W. A. Coghlan, D. S. Easton, C. C. Koch, and J. O. Scarbrough, *J. Appl. Phys.* **53**, 1445 (1982).

<sup>18</sup>H. S. Råde, *Feinwerktechnik Messtechnik* **83**, 230 (1975).

<sup>19</sup>G. R. Stewart and A. L. Giorgi, *Phys. Rev. B* **17**, 3534 (1978).

<sup>20</sup>R. E. Schwall, R. E. Howard, and G. R. Stewart, *Rev. Sci. Instrum.* **46**, 1054 (1975).

<sup>21</sup>A. J. Bevolto, *Cryogenics* **14**, 661 (1974).

<sup>22</sup>M. Wun and N. E. Phillips, *Cryogenics* **15**, 36 (1975).

<sup>23</sup>D. W. Osborne, H. E. Flotow, and F. Schreiner, *Rev. Sci. Instrum.* **38**, 159 (1967).

<sup>24</sup>W. L. McMillan, *Phys. Rev.* **167**, 331 (1967).

<sup>25</sup>C. C. Koch, D. M. Kroeger, J. O. Scarbrough, and B. C. Giessen, *Phys. Rev. B* **22**, 5213 (1980).

<sup>26</sup>W. L. Johnson, *J. Phys. (Paris) Colloq.* **41**, C8-731 (1980).

<sup>27</sup>For an experimental study of specific-heat measurements in a material consisting of two closely coupled superconducting phases, see J. Lechevet, J. E. Neighbor, and C. A. Schiffman, *J. Low. Temp. Phys.* **27**, 407 (1977).

<sup>28</sup>S. J. Poon, *Phys. Rev. B* **27**, 5519 (1983).

<sup>29</sup>D. M. Kroeger, C. C. Koch, C. G. McKamey, and J. O. Scarbrough, in *Proceedings of the Fifth International Conference on Liquid and Amorphous Metals, Los Angeles, California, August, 1983* [*J. Non-Cryst. Solids* (to be published)].

<sup>30</sup>M. Sakata, N. Cowlam, and H. A. Davies, *J. Phys. F* **11**, L157 (1981).

<sup>31</sup>C. N. J. Wagner and D. Lee, *J. Phys. (Paris) Colloq.* **41**, C8-242 (1980).

<sup>32</sup>Y. D. Dong, G. Gregan, and M. G. Scott, *J. Non-Cryst. Solids* **43**, 403 (1981).

<sup>33</sup>K. H. J. Buschow and N. Beekmans, *Phys. Rev. B* **19**, 3843 (1979); K. H. J. Buschow, B. H. Verbeek, and A. G. Dirks, *J. Phys. D* **14**, 1087 (1981).

<sup>34</sup>M. G. Scott, G. Gregan, and Y. D. Dong, in *Proceedings of the Fourth International Conference on Rapidly Quenched Metals, 1981, Sendai, Japan*, Ref. 4, Vol. II, p. 671.

<sup>35</sup>Y. Nishi, T. Morohoshi, M. Kawakami, K. Suzuki, and T. Masumoto, in *Proceedings of the Fourth International Conference on Rapidly Quenched Metals, 1981, Sendai, Japan*, Ref. 4, p. 111.

<sup>36</sup>S. R. Nagel and J. Tauc, *Phys. Rev. Lett.* 35, 380 (1975).

<sup>37</sup>M. E. Kirkpatrick, D. M. Bailey, and J. F. Smith, *Acta Crystallogr.* 15, 252 (1962).